
Article:
Brunelli, M., Perrault, C.M. orcid.org/0000-0003-2230-6994 and Lacroix, D. orcid.org/0000-0002-5482-6006 (2017) Mechanical response of 3D Insert® PCL to compression. Journal of the Mechanical Behavior of Biomedical Materials, 65. pp. 478-489. ISSN 1751-6161

https://doi.org/10.1016/j.jmbbm.2016.08.038

Mechanical response of 3D Insert® PCL to compression

M. Brunelli, C.M. Perrault, D. Lacroix

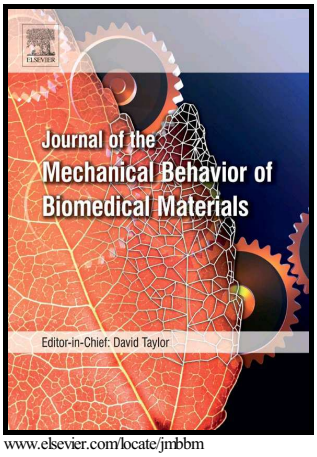

www.elsevier.com/locate/jmbbm

PII: S1751-6161(16)30328-9
DOI: http://dx.doi.org/10.1016/j.jmbbm.2016.08.038
Reference: JMBBM2078

To appear in: *Journal of the Mechanical Behavior of Biomedical Materials*

Received date: 13 July 2016
Revised date: 25 August 2016
Accepted date: 26 August 2016

Cite this article as: M. Brunelli, C.M. Perrault and D. Lacroix, Mechanica response of 3D Insert® PCL to compression, *Journal of the Mechanica Behavior of Biomedical Materials* http://dx.doi.org/10.1016/j.jmbbm.2016.08.038

Mechanical response of 3D Insert® PCL to compression

M. Brunelli [1], C.M. Perrault [1]**, D. Lacroix [1]****

[1] INSIGNEO Institute for in silico medicine, Department of Mechanical Engineering, University of Sheffield, UK

**email:* m.brunelli@sheffield.ac.uk

***email:c.perrault@sheffield.ac.uk*

****Corresponding author*

Address: Dept. Mechanical Engineering,
The University of Sheffield
Pam Liversidge Building - Room F32
Mappin Street
S1 3JD Sheffield, United Kingdom

email: d.lacroix@sheffield.ac.uk

ABBREVIATIONS

3D	three dimensional
2D	two dimensional
3D PCL	3D Insert PCL
d	Displacement
DMA	Dynamic mechanical analysis
E'	Storage modulus
E''	Loss modulus
E_a	apparent elastic modulus
F	Load
GV	Grey values
µCT	Micro computed tomography
n	Number of samples
PBS	Phosphate buffered saline
PDMS	Polydimethylsiloxane

ROI	Region of interest
SEM	Scanning electron microscopy
TE	Tissue engineering
V_{mat}	Volume of material
V_{ROI}	Volume in ROI

1 Introduction

Tissue Engineering (TE) approach aims at closely mimicking the biological environment found in the body to drive progenitor cells toward a defined differentiation pathway and to obtain fully functional tissue as replacement for injured sites. While the behaviour of cellular lineages seeded on two dimensional (2D) surfaces is nowadays well defined on a wide range of materials [1], this culture method does not appropriately mimic the biological environment because it lacks 3D structure. As a consequence, one of the first challenges addressed by TE regards the possibility of employing structures closely mimicking the geometry and chemistry of the biological environment found in the target tissue. For bone regeneration purposes, a basic requirement is for the scaffold to be able to bear mechanical stimuli, as bone is often under mechanical load by the action of muscles and body movements. Synthetic materials made by polymerization of lactic acid, glycolic acid or caprolactone were explored to manufacture composite scaffolds, often embedding natural proteins. This approach led to the fabrication of scaffolds able to bear mechanical forces, providing at the same time an architecture and a matrix similar to the bone tissue niche [2]. Among those, polycaprolactone (PCL), a thermoplastic polymer with low glass transition and low melting temperature [3], is gaining interest as temperature dependent processes can be employed to shape it, enabling control over features at micro scale [4]–[6]. PCL was also shown to be biocompatible [7] and have slow degradation rates due to its high degree of crystallinity and hydrophobicity [8], [9]. These characteristics make PCL highly suitable for studies requiring consistency in the mechanical properties of the material over time [10]. Moreover, PCL is increasingly proposed as product for in vivo tissue regeneration [11]. As consequence, its suitability to be used for medical purposes needs to be verified [12]. FDA regulations [13] aim to define standards for guaranteeing safety of human medical grade products to be launched on the market. On the respect of these rules, the device must at last satisfy the user needs and in this particular paper we address issues related to repeatability of commercially available PCL scaffolds in terms of architecture and mechanical response.

Indeed, the architecture of scaffolds showed to strongly impact the mechanical properties of polymeric scaffolds [14]–[17], as consequence here micro-computed tomography (µCT) is used a non-destructive approach to study scaffolds geometry. In order to obtain

reproducibility of the response to compression, pre-stresses existing in the scaffolds must be prevented. For this purpose, static pre-conditioning was proposed in multiple studies [18]–[20] as a method to prevent progressive relaxation of the structure undergoing dynamic cycles. Environmental conditions are known to affect the mechanical response of scaffolds [21] as demonstrated by Dynamic Mechanical Analysis (DMA) in previous literature studies [14], [15], [17]. DMA was used in this study to capture any difference in the mechanical response of scaffolds when surrounded by liquid (water). The aims of this study were to characterize the mechanical response of 3D PCL scaffolds to compression and to assess the variability of the mechanical response to architectural variability and sample repositioning.

2 Materials and Methods

2.1 Scaffolds and micro computed tomography

3D Insert PCL scaffolds (Biotek, USA) 5 mm in diameter and 1.5 mm tall were stacked one upon another (up to three samples) into a straw and separated by small pieces of paper. Then, they were placed on a holder located in the µCT equipment between the x-ray source and the detector (Skyscan 1172, Belgium). Scaffolds were scanned at 40 kV, 10 W and 250 mA. No filters were applied and the pixel size was set to 17.4 µm. During the scanning, scaffolds were automatically rotated and consecutive projection images were acquired by the detector. Through algorithms implemented in the CTAn reconstruction software (Bruker, Belgium), projections were automatically analysed, and cross-sectional slices showing the density profile of the material were provided. Such 2D slices were obtained by applying ring artefacts and beam hardening corrections of respectively 10% and 15%. From the histogram, grey values (GV) between 0 and 0.2 were selected to improve image contrast.

2.2 SEM

A 3D PCL sample was stuck to the top surface of a cylindrical holder by a carbon sticker. After undergoing gold sputtering for 5 minutes, pictures were acquired by SEM at 15 KV.

2.3 Geometric variability

According to histograms obtained by µCT scans, grey values between 8,000 and 13,000 were selected to compute a mask of scaffolds (n=14) architecture and quantify volume, surface area and porosity. Volume and surface area were calculated automatically by Simpleware on the overall mask while porosity measurements required the selection of an

internal ROI. The percentage of material (V_{mat}) occupying the overall selected volume (V_{ROI}) was considered in the estimation of the final porosity (Eq. 1) and the relative density (Eq. 2).

$$p=1-(V_{mat}/V_{ROI})*100 \quad \text{Eq. 1}$$

$$RD=100-p \quad \text{Eq. 2}$$

3D volumes were further elaborated in ImageJ (NIH, USA) to evaluate the average fiber diameter. Fiber diameter was measured on a cross-section of the scaffold whose cutting plane passes through the centroid of the structure. Then, circular areas were drawn matching the fibers profile. Other parameters taken into account were the height and the mass of scaffolds measured respectively using a calliper (Mitutoyo, UK) and a digital scale (Kern & Sohn GmbH, Germany).

2.4 Stress/strain curve

Stress/strain curves were obtained applying loading ramps at 5, 8 and 14% compressive strain at 10 µm/s using a BOSE Biodynamic System 5500 (BOSE Corp., USA) in order to determine a range of strain avoiding plastic deformation. Scaffolds (n=5) were tested at 25°C in air and at 40% of humidity. The zero position was defined by load referring to an initial preload of 0.1 N on the structure as zero stress/strain condition. Such value corresponded to the minimum variation detectable by the load sensor. Load (F) and displacement (d) data were acquired at 20 Hz using the Wintest 7.0 software (BOSE Corp., USA). The engineering uniaxial stress and strain were calculated.

2.5 Sample preconditioning and dynamic compression

Scaffold relaxation was obtained by static preconditioning. A 8% compressive ramps was applied at 10 µm/s and the resulting displacement was kept constant for 3 h (Fig. 1). To confirm the absence of relaxation after static preconditioning, samples (n=3) underwent cyclic compression before and after relaxation at 37°C and 40% humidity. Dynamic forces were applied as 5% strain triangle waves for 10 times at 1 Hz (Fig. 2).

2.6 Apparent elastic modulus

5% strain ramps at 10 µm/s were applied at 25, 30 and 37°C allowing stabilization of the temperature inside the incubator for 30 min at each temperature variation. Samples (n=3) were tested with 10 ramps and recovery of the scaffold was achieved by allowing 10 min recovery between consecutive ramps. The apparent elastic modulus was calculated as

average of stress/strain ratio in the range of linear response of scaffolds, hence where the secant modulus was constant.

2.7 Dynamic mechanical analysis

Samples (Table 1) were preloaded at 0.1 N and a ramp at 5% strain was superimposed to induce a pre-stress on the structures. Consecutive sinewaves 2% peak to peak were applied at 0.1, 0.5, 1, 5, 10 Hz. The storage modulus (*E'*) gives insight of the elastic response of the structure and of the energy stored by the specimen while the loss modulus (*E''*) takes into account the dissipation effects caused by the viscoelastic component. The two moduli can be combined to obtain the complex elastic modulus (Eq.3) and tan δ (Eq.4).

$$E^* = E' + iE'' \quad \text{Eq. 3}$$

$$\tan\delta = E''/E' \quad \text{Eq. 4}$$

DMA was performed in dry or wet conditions keeping samples (n=3) respectively in air or water at 37℃. The protocol was controlled by the DMA software (BOSE Corp., USA) and post processing of data was automatically provided by the DMA Analysis software (BOSE Corp., USA). DMA analysis was repeated three times on the same sample to determine *E'*, *E''* and tan δ without varying the orientation of the scaffold in the machine.

2.8 Boundary effects and mechanical variability

The effect of geometry and porosity on the response to compression was first investigated on a mechanically well-known material such as polydimethylsiloxane (PDMS, Sylgard 184 Dow Corning, US) in an effort to provide reference measurements. PDMS was prepared by mixing curing agent and monomer at 1:10 (w/w) ratio. Vacuum was applied until complete removal of bubbles and PDMS was cured at 75℃ for 20 min in a temperature controlled oven. Once solidified, PDMS was cut into a cylindrical shape by punching holes 5 mm in diameter through the structure. Through this procedure, it was possible to obtain PDMS samples whose dimensions match 3D PCL. PDMS and 3D PCL mechanical properties were tested by applying a preload of 0.1 N followed by a 5% strain loading ramp at a fixed velocity. E_a values obtained by performing 10 ramps were averaged to perform statistical analysis and allowing 10 min recovery between consecutive ramps. In this study the effect of three variables on the mechanical response of samples were studied: height, velocity and sample orientation. The first was explored to test the existence of a link between the height of the specimen and its measured mechanical properties.

For this purpose, PDMS samples (n=3) 2 mm (PDMS2) and 10 mm (PDMS10) height were tested under the same conditions in terms of strain amplitude and rate. To evaluate the adaptation of the material when displacement was applied at different rates, the velocity of the loading ramp was varied at 1 and 10 µm/s on both PDMS2 and 3D PCL. The 3D PCL samples (n=3) used in the experiments were chosen randomly from the same batch (Table 1). The last variable considered was the orientation of the sample on the radial plane. At each velocity, E_a was statistically analysed to evaluate the effect elicited by rotating the sample on the *xy* plane and around the *z* axis on a compact or a 3D porous material. Statistical analysis was performed by SPSS software. Normality and equality of variances among series of data were tested by Shapiro and Levene test, and ANOVA statistical analysis was performed.

3 Results

3.1 Micro-computed tomography and 3D PCL architecture

Scaffold architecture is believed to play a central role in the variability of the mechanical response when compressing different samples. For this reason, each scaffold was scanned by µCT prior to dynamic compression and the geometrical features were scrutinized to identify any significant difference among scaffolds (Fig.4A). All parameters tested (Table3) showed high deviation from the average value with percentage error up to 12%. The average scaffold height was 1.56 mm, with a range from 1.36 to 1.67 mm. Numerical reconstruction of the samples showed that the differences in height were due to the dimension of fibers varying within the sample and among different specimens. All samples also presented with misalignment between fibers, imperfections in the structure and variable pore size. In particular, SEM pictures helped confirming fusion phenomena occurring between fibers located in consecutive layer placed on the z plane (Fig 4B). Fibers also showed a lack of cylindricity, irregular spacing and a highly variable diameter (Fig.4C). In the same sample, the diameter of fibers varied up to 8% while, extending the comparison among different samples, the variability increased up to 12%. Beyond scaffold height and fiber diameter, parameters with variability above 10% include surface area, volume and porosity of 11.3%, 12.8% and 15.6%, respectively.

3.2 Stress/strain curve and apparent elastic modulus

The stress/strain curve (Fig.3A) shows a classic viscoelastic behaviour, identified by the non-linear increase of stress with increasing strain. Moreover, the development of an hysteresis cycle suggests loss of energy associated to the deformation. Indeed, the unloading curve showed 6% residual strain when a single ramp at 14% strain was applied, suggesting the occurrence of plastic deformation of the structure for strains above 8%. Applying a 8% strain (Fig.3B), the plastic deformation occurred to be below 2% which

corresponds to the precision of the displacement sensor of the mechanical testing machine. As consequence, plastic effect can be considered null and 8% was selected for inducing relaxation of each scaffold before testing. A single 5% strain ramp (Fig.3B) did not present plastic effects and showed complete recovery of the structure. For this reason, low strain values thresholded at 5% were applied for testing the behaviour of samples under compression after relaxation. At this point, the secant modulus was examined as it remains constant in the range of strain governed by linearity on the stress/strain curve (Fig.3C). Following these findings, a certain strain was considered as belonging to the linear range if the secant modulus underwent a maximum variation of 10% from the value observed at 1%. As a result, all secant moduli falling in the range of strain between 1 and 2.5% were averaged and defined as apparent elastic modulus. E_a remained constant among stimulations regardless of the previous history of the material if (1) the strains applied previously did not exceed the 8% threeshold for plastic deformation; (2) samples were not repositioned in the machine; and (3) samples were allowed to recovery for 10 min between consecutive compression cycles. E_a was found to decrease linearly with increasing temperature (Fig.5A). Samples tested at 25, 30 and 37°C showed E_a respectively at 4.8, 3.8 and 2.2 MPa (Fig.5B).

3.3 Preconditioning and viscoelastic effects

Viscoelastic effects occurred when cyclic loading was applied, enhancing progressive relaxation (Fig.6A) as the structure was not allowed to recover between ramps. The highest dissipation of energy was observed during the first cycle. Samples required an average of 150 min to completely relax under 8% strain compression, reaching a plateau (Fig.6B). When applying cyclic loading on statically preconditioned specimens, relaxation was absent and compression tests showed overlapping loading/unloading curves (Fig.6C). The absence of plastic deformation was confirmed as no residual strain was observed at the end of the unloading curve. Despite the similarity in the relaxation pattern, the load force registered by the machine varied among samples although the same strain was applied, suggesting geometrical differences play a role in the mechanical response of scaffold to compression.

3.4 Mechanical characterization of PDMS

PDMS samples with different heights underwent the same compressive protocol as 3D PCL to evaluate the effect of height on the response of the material. At first glance, height seemed to play a fundamental role on the mechanical response, while rate of application of the stimuli did not elicit any strong effect on a compact material as PDMS (Fig.7). Statistical analysis was performed to test data for normality and equality of variances. Data series presented a normal distribution and equal variance as demonstrated respectively by the Shapiro and Levene's test (Table 3). Comparing samples of same height by ANOVA (Table 3) showed no significant differences in the mechanical response. This confirms the suitability of PDMS as reference material and evaluation of the precision of the methodology and quantification of the human and systematic error. Despite the repeatability in the measure of the material stiffness for a given height suggested by the low standard deviation, PDMS10 showed a significantly higher E_a ($p<0.001$) compared to PDMS2 (Table 4). This suggests

that a shorter height causes an underestimation of the final apparent elastic modulus. T-Test statistics showed no significant difference for a single PDMS2 sample compressed first at 1 µm/s and then at 10 µm/s when its orientation in the machine was varied (Table 4).

3.5 3D PCL variability analysis

Compression of 3D PCL scaffolds showed a different behaviour, due to the texture of the architecture and the absence of a compact material. When testing the scaffolds under the same condition than for PDMS samples, random variation in the mechanical response was observed. Indeed, stress/strain curves did not overlap when a single 3D PCL sample was compressed several times varying its orientation of the sample in the machine (Fig.7). Despite of this, the average percentage error resulting from the application of a defined compression protocol remained constant among specimens, amounting to 1 MPa. However, the overall error reached up to 30% of the measure depending on the E_a values associated with the mechanical response of samples to compression. Contrary to PDMS, 3D PCL showed differences in the overall mechanical response when different samples were tested (Fig.8) as already noticed during relaxation. According to Shapiro test, data series followed a non-normal distribution (Table5) for samples A and B compressed respectively at 1 and 10 µm/s. However, a further analysis on boxplot diagrams was performed, revealing symmetry especially at 10 µm/s (Fig.9).

Following those outcomes, data series were considered as normally distributed while the presence of outliers was associated to human error occurring during the application of the initial pre-load. Unlike PDMS samples, one out of three 3D PCL samples showed differences in the mechanical response when compressed at different velocity (Table5). Indeed, sample C resulted significantly stiffer ($p<0.05$) when compressed at 10 µm/s, suggesting velocity as a variable in the mechanical response of porous materials. Tukey post-hoc test (Table 5) showed significant differences ($p<0.05$) between samples A, B and B, C at 1 µm/s.

The differences in the mechanical response of samples became less evident at higher velocity as the mean value varied only comparing samples B and C with probability values falling close to the statistically significant threshold (Table 5). These findings highlight once more the importance of height and architecture in the definition of the mechanical response of the material. Despite the difference in the average E_a, the homogeneity of variances between series of data was obtained by Levene's test regardless of the sample architecture (Table 6), allowing to define 1 MPa as the maximum standard deviation acceptable.

3.6 DMA analysis

Air and water were taken as variables in this study to define the effect of a different surrounding environment on mechanical behaviour of 3D PCL. No significant differences were found when testing the same sample in dry or immersed state. Indeed, storage modulus, loss modulus and tan δ remained constant regardless of the environment (Fig.10). For all samples, increasing frequency above 5 Hz led to significant increase

($p<0.05$) in storage modulus and a significant decrease ($p<0.05$) in tan δ. Variations in terms of loss modulus were observed just on one sample out of three, showing less dissipation effects with increased frequency.

4 Discussion

4.1 3D PCL apparent elastic modulus

Stress/strain curves showed a viscoelastic, non-linear behaviour. E_a calculated as average in the range of strain between 1-2.5% amounted to 2.2±1 MPa at 37°C. Such value classifies the 3D PCL as a good substitute for bone recovery as it matches the Young's modulus of fibrous tissue developing during early stage of healing and marrow [22]. However, an underestimation of the real value in terms of stiffness of the material is believed to occur due to the limited height of scaffolds, as demonstrated by applying the same conditions on PDMS samples at different height. Despite this, E_a remained constant loading a single sample which did not undergo repositioning in the machine.

The repeatability of E_a enabled the investigation of the effect of temperature variation on the 3D PCL stiffness. The dependence noticed between mechanical response to compression over temperature can be explained by the polymeric nature of the scaffolds [23], as polymers becomes softer at higher temperature due to the weaker bonds between adjacent polymeric chains. These thermal properties were previously reported for PCL scaffolds tested either as a compact [24], [25] or a 3D structure [14], [16].

Comparison between samples was difficult because of the variation in the scaffold architecture, a parameter known to affect mechanical response. Numerous studies [14], [15], [26] have shown a strict correlation between porosity, pore size, offset between fibers and mechanical response. These parameters together with other properties of the sample - such as the geometry, degree of crosslinking and molecular weight - should be taken into account when comparing results with the literature (Table 7). For example, the stiffer E_a values found by Hutmacher [14] could be due to the different 3D geometry of their scaffolds, as well as to the molecular weight of the raw material (43,000-50,000 Da for 3D PCL). Despite similar geometries, Yeo et al. [16] found a higher modulus than for 3D PCL. This could be due to the different laydown pattern as well as the inclusion of TCP particles in the structure. The stiffness of PCL scaffolds with similar geometry was tested by Sobral [15], who evaluated the mechanical response of scaffolds with pore size varying between 100 and 750 μm and found a Young's modulus ranging between 1.5 and 8 MPa. Assuming that the variability in pore size of 3D PCL samples matched that of the other geometrical features such as height, porosity, fiber diameter, surface area and volume, the pore size of 3D PCL can be reported as 300±48 μm, with a maximum error of 15.6% from the average value provided by the manufacturer. As a consequence, the E_a values in this study are in agreement with Sobral's [15]. Moreover, the percentage error of the average stiffness in the literature reaches 14% when consecutive identical compression cycles are applied on different samples. The deviation from the average value was instead higher in this study because of architectural

differences and imperfections which lead to high variability in the 3D PCL mechanical response.

4.2 Mechanical response and geometry

Before dynamic testing, samples underwent static preconditioning to induce stabilization of the structure and to guarantee reproducibility of the stimuli when several loading cycles are applied. Due to the absence of plastic deformation noticed applying loading ramps at 8% of strain, such value was used to induce complete relaxation from pre-stresses on all samples before further mechanical testing. PCL scaffolds with an architecture similar to 3D PCL relaxed under constant strain conditions over periods ranging from few hundreds of seconds [19] up to 33 min [20], while requiring about 180 min in this study. The differences with the literature are believed to be due to the molecular weight and the degree of crystallinity of samples [27]. The effect of degradation on the response of scaffolds to mechanical stimuli was not considered in this paper because experiments were performed over a period of time during which PCL scaffolds exposed to air or water were proved to not be affected by degradation [9], [21]. Despite the consistent response during dynamic compression, the overall stress varied among scaffolds due to differences in the geometry and the architecture. As shown by µCT reconstructions, fibers presented different dimensions and seemed to be fused together, randomly decreasing the spacing between layers in the z-plane. This variability caused significant differences in the porosity distribution and interconnectivity within samples. Moreover, the height of 3D PCL does not meet the requirements for reliable estimation of the elastic modulus, stating the height to be at least twice the diameter [28]. Consequently, boundary effects occurred, leading to differences in the mechanical response when the orientation α of the same sample was varied. In addition, scaffolds often present a bullet-like shape due to the fabrication method which involves punching cylindrical shaped scaffolds from large sheets of polymeric fibers produced by fused deposition modelling. This fabrication method not only caused imperfection in the overall shape of scaffolds but it which often caused fusion between consecutive fibers as showed here by SEM imaging due to the high temperatures required in the process. In order to understand the contribution of the geometrical variability of samples loaded in different orientations, PDMS was used as reference material. Our results showed that some error can be associated with (1) a systematic component associated to the accuracy of displacement and load sensors, and (2) human error lessen by routine and well-established procedures but limited by human eye resolution. This error can still be considered as minimal, given that it was found to be below 10% regardless of the sample orientation. As a consequence, the high variability up to 30% found with the 3D PCL response can be assumed to be related to the geometry and architecture of samples. Contrary to biological tissue and the 3D PCL, these findings show that the velocity of application of the stimuli and the orientation in the machine do not elicit any effect on the mechanical response of samples for a compact and elastic material such as PDMS. Variances remained consistent among different samples or varying testing conditions with standard deviation values below ± 0.2 MPa regardless of velocity, height and repositioning of the sample. We concluded that this value was considered representative of the standard deviation caused by the human and systematic error.

4.3 DMA and stress distribution

DMA analysis defined the effect of different frequencies on 3D PCL mechanical response and helped with the evaluation of viscous and elastic properties of the structure. Increasing frequencies led to an increase in the ability of the scaffold to store energy as noticed by the increase in storage modulus and the simultaneous decrease of tan δ affecting all samples. Scaffolds with interconnectivity and geometry very similar to 3D PCL samples but higher height were demonstrated to follow the same pattern in terms of *E'* and tan δ. According to Sobral study [15], the differences observed comparing *E'* among samples can be addressed to larger pores characterizing sample S4. Moreover, *E'* was lower for all conditions tested compared to our findings because of the difference in the amplitude of the sinewave applied. Indeed, the amplitude of the strain at the peak of compression amounted to 6% in our experiment, compared to 1.4% in the literature.

A cylindrical geometry matching PCL scaffolds presented here was investigated by Yilgor [17], although the height of the specimens and the protocol applied to samples during the DMA analysis were unclear. Storage modulus and tan δ values match the results found in our study when a laydown pattern of 0/90° is considered. Among others, DMA enabled also the investigation of the effect elicited by the external environment on the mechanical response of 3D PCL. No significant differences were observed comparing *E'*, *E''* and tan δ in air or in liquid. These results match findings in the literature related to five-layered pattern structures [14], while slightly different three-layered architectures, tested in the same study, were found to decrease stiffness upon immersion in PBS.

4.4 3D Insert PCL as a mechanical in vitro model

This study aims to verify the geometrical repeatability of 3D PCL scaffolds and investigate their mechanical response to compression in order to evaluate the possibility of employing 3D PCL as in vitro model for repeated mechanical stimulation of cells. The main challenge at this stage consisted in defining E_a providing a good representation of the linear response to compression due to the variable architecture of scaffolds. At first, progressive relaxation of the structure was achieved by static preconditioning samples at 8% compressive strain. Once relaxed, a range of strains eliciting an elastic response was identified for further analysis of the mechanical behaviour of 3D PCL varying temperature, or under cyclic load. The main drawback in the evaluation of the stiffness of the structure was related to the high variability in the measurement. Indeed, considering a different orientation on the xy plane, the same scaffold led to varying up to 30% from the average value. This variation was much higher than the percentage error found applying the same protocol to standard PDMS samples with identical geometry but compact architecture. This difference between the two materials suggests a link between the architecture of 3D PCL and the variability of the measure. As extensively claimed in the literature [14], [15], [17], the mechanical properties of scaffolds vary greatly depending on the diameter of the fibers, their relative orientation or the presence of defects. As observed by µCT, 3D PCL is characterized by many structural

irregularities which cause a highly randomized distribution of stresses. Furthermore, the sample height is three-fold lower than the diameter, causing an underestimation of the overall stiffness of the structure as demonstrated compressing PDMS samples with different height. The variability observed in the mechanical response of 3D PCL can be also considered advantageous in an effort to simulate the in vivo environment. Indeed, the bone fracture site is characterized by a combination of tensile, compressive and bending forces strictly connected to the synergic action of muscles, tendons, blood flow and external factors, rather than a single and uniform compressive component.

5 Conclusions

3D PCL scaffolds demonstrated a high variability in their architecture and, as consequence, also in the mechanical response. Despite of this, this study helped quantifying an apparent Young's modulus for 3D PCL of 2.2 MPa at 37°C. Moreover, the maximum variation was established to reach at worst the 30% of the average E_a considering a wide population of scaffolds. E_a defined among 1 and 2.5% strain remained constant among stimulations, allowing the investigation of a relationship between temperature and 3D PCL mechanical response. E_a was also found to consistently vary repositioning the same scaffold or comparing different specimens because of boundary effects related to the small height and differences in architecture. The findings of this study confirm the suitability of 3D PCL to be used for bone mechanobiology studies although 3D PCL was demonstrated to provide a high variability in the mechanical response to compression. Importantly the extensive mechanical characterisation of those scaffolds show the variability encountered from sample to sample and the importance of controlling and characterising parameters such as pore architecture, temperature and strain rate. Data obtained by this study are currently used for the development of computational models aiming to establish the local distribution of stresses and fluid flow [29] within the structure and give a much clearer representation of forces when 3D porous scaffolds undergo external compression.

Acknowledgments

Funding: This work was supported by the European Research Council [grant number FP7-258321].

References

[1] A. J. Engler, S. Sen, H. L. Sweeney, and D. E. Discher, "Matrix Elasticity Directs Stem Cell Lineage Specification," *Cell*, vol. 126, no. 4, pp. 677–89, 2006.

[2] G. Chen, T. Ushida, and T. Tateishi, “Scaffold Design for Tissue Engineering,” *Macromol. Biosci.*, vol. 2, no. 2, pp. 67–77, 2002.

[3] M. E. Hoque, D. W. Hutmacher, W. Feng, S. Li, M.-H. Huang, M. Vert, and Y. S. Wong, “Fabrication using a rapid prototyping system and in vitro characterization of PEG-PCL-PLA scaffolds for tissue engineering,” *J. Biomater. Sci. Polym. Ed.*, vol. 16, no. 12, pp. 1595–1610, 2005.

[4] D. Rohner, D. W. Hutmacher, T. K. Cheng, M. Oberholzer, and B. Hammer, “In vivo efficacy of bone-marrow-coated polycaprolactone scaffolds for the reconstruction of orbital defects in the pig.,” *J. Biomed. Mater. Res. Part B*, vol. 66, pp. 574–80, 2003.

[5] J. M. Williams, A. Adewunmi, R. M. Schek, C. L. Flanagan, P. H. Krebsbach, S. E. Feinberg, S. J. Hollister, and S. Das, “Bone tissue engineering using polycaprolactone scaffolds fabricated via selective laser sintering,” *Biomaterials*, vol. 26, no. 23, pp. 4817–827, 2005.

[6] S. J. Hollister, “Porous scaffold design for tissue engineering.,” *Nat. Mater.*, vol. 4, no. 7, pp. 518–24, 2005.

[7] G. G. Pitt, M. M. Gratzl, G. L. Kimmel, J. Surles, and a Sohindler, “Aliphatic polyesters II. The degradation of poly (DL-lactide), poly (ε-caprolactone), and their copolymers< i> in vivo</i>,” *Biomaterials*, vol. 2, no. 4, pp. 215–220, 1981.

[8] M. Chasin and R. Langer, *Biodegradable Polymers as Drug Delivery Systems*. New York: M. Dekker, Inc., 1990.

[9] C. X. F. Lam, D. W. Hutmacher, J.-T. Schantz, M. A. Woodruff, and S. H. Teoh, “Evaluation of polycaprolactone scaffold degradation for 6 months in vitro and in vivo.,” *J. Biomed. Mater. Res. A*, vol. 90, no. 3, pp. 906–919, 2009.

[10] L. J. Gibson and M. F. Ashby, *Cellular solids: structure and properties*. 1999.

[11] J. T. Schantz, T. C. Lim, C. Ning, S. H. Teoh, K. C. Tan, S. C. Wang, and D. W. Hutmacher, “Cranioplasty after trephination using a novel biodegradable burr hole cover: technical case report.,” *Oper. Neurosurg.*, vol. 58, no. 1, 2006.

[12] M. P. Chhaya, P. S. Poh, E. R. Balmayor, M. van Griensven, J. T. Schantz, and D. W. Hutmacher, “Additive manufacturing in biomedical sciences and the need for definitions and norms.,” *Expert Rev. Med. Devices*, 2015.

[13] R. J. Morrison, K. N. Kashlan, C. L. Flanangan, J. K. Wright, G. E. Green, S. J. Hollister, and K. J. Weatherwax, “Regulatory Considerations in the Design and Manufacturing of Implantable 3D-Printed Medical Devices,” *Clin. Transl. Sci.*, vol. 8, no. 5, pp. 594–600, 2015.

[14] D. W. Hutmacher, T. Schantz, I. Zein, K. W. Ng, S. H. Teoh, and K. C. Tan, “Mechanical properties and cell cultural response of polycaprolactone scaffolds designed and fabricated via fused deposition modeling.,” *J. Biomed. Mater. Res.*, vol. 55, no. 2, pp. 203–16, May 2001.

[15] J. M. Sobral, S. G. Caridade, R. Sousa, J. F. Mano, and R. L. Reis, “Three-dimensional plotted scaffolds with controlled pore size gradients: Effect of scaffold geometry on mechanical performance and cell seeding efficiency.,” *Acta Biomater.*, vol. 7, no. 3, pp. 1009–18, Mar. 2011.

[16] A. Yeo, B. Rai, E. Sju, J. J. Cheong, and S. H. Teoh, “The degradation profile of novel , bioresorbable PCL – TCP scaffolds : An in vitro and in vivo study,” *J. Biomed. Mater.*

Res. Part A, vol. 84, no. 1, pp. 208–18, 2007.

[17] P. Yilgor, R. Sousa, R. L. Reis, N. Hasirci, and V. Hasirci, "3D plotted PCL scaffolds for stem cell based bone tissue engineering," *Macromol. Symp.*, vol. 269, no. 1, pp. 92–99, 2008.

[18] J. M. Cloyd, N. R. Malhotra, L. Weng, W. Chen, R. L. Mauck, and D. M. Elliott, "Material properties in unconfined compression of human nucleus pulposus, injectable hyaluronic acid-based hydrogels and tissue engineering scaffolds," *Eur. Spine J.*, vol. 16, no. 11, pp. 1892–98, 2007.

[19] J. Xie, M. Ihara, Y. Jung, I. K. Kwon, S. H. Kim, Y. H. Kim, and T. Matsuda, "Mechano-Active Scaffold Design Based on Microporous Poly (L-lactide-co-ε-caprolactone) for Articular Cartilage Tissue Engineering: Dependence of Porosity on Compression Force-Applied Mechanical Behaviors," *Tissue Eng.*, vol. 12, no. 3, pp. 449–59, 2006.

[20] P. K. Valonen, F. T. Moutos, A. Kusanagi, M. G. Moretti, B. O. Diekman, J. F. Welter, A. I. Caplan, F. Guilak, and L. E. Freed, "In vitro generation of mechanically functional cartilage grafts based on adult human stem cells and 3D-woven poly(ε-caprolactone) scaffolds," *Biomaterials*, vol. 31, no. 8, pp. 2193–200, 2010.

[21] C. X. Lam, M. M. Savalani, S. H. Teoh, and D. W. Hutmacher, "Dynamics of in vitro polymer degradation of polycaprolactone-based scaffolds: accelerated versus simulated physiological conditions," *Biomed Mater*, vol. 3, no. 3, p. 34108, 2008.

[22] D. Lacroix, P. J. Prendergast, G. Li, and D. Marsh, "Biomechanical model to simulate tissue differentiation and bone regeneration: Application to fracture healing," *Med. Biol. Eng. Comput.*, vol. 40, no. 1, pp. 14–21, Jan. 2002.

[23] I. M. Ward and J. Sweene, *Mechanical Properties of Solid Polymers*. John Wiley & Sons, Ltd, 2012.

[24] F. Yoshii, D. Darwis, H. Mitomo, and K. Makuuchi, "Crosslinking of poly(epsilon-caprolactone) by radiation technique and its biodegradability," *Radiat. Phys. Chem.*, vol. 57, no. 3–6, pp. 417–20, 2000.

[25] L. Averous, L. Moro, P. Dole, and C. Fringant, "Properties of thermoplastic blends: Starch-polycaprolactone," *Polymer (Guildf).*, vol. 41, no. 11, pp. 4157–4167, 2000.

[26] S. Ghosh, V. Gutierrez, C. Fernández, M. Rodriguez-Perez, J. C. Viana, R. L. Reis, and J. F. Mano, "Dynamic mechanical behavior of starch-based scaffolds in dry and physiologically simulated conditions: Effect of porosity and pore size," *Acta Biomater.*, vol. 4, no. 4, pp. 950–59, 2008.

[27] R. F. Landel and L. E. Nielsen, *Mechanical properties of polymers and composites*. CRC Press, 1993.

[28] B. Gama, S. L. Lopatnikov, and J. W. Gillespie, "Hopkinson bar experimental technique: A critical review," *Appl. Mech. Rev.*, vol. 57, no. 4, pp. 223–51, 2004.

[29] A. Campos Marin and D. Lacroix, "The inter-sample structural variability of regular tissue-engineered scaffolds significantly affects the micromechanical local cell environment," *Interface Focus*, vol. 5, no. 2, pp. 20140097–20140097, 2015.

List of figures

Fig. 1: relaxation protocol performed maintaining constant strain for 180 min.
Fig. 2: Cyclic compression applied before and after relaxation of 3D PCL to test the viscoelastic response of scaffolds.
Fig. 3: Stress/strain curve applying loading/unloading ramp to evaluate 3D PCL response to mechanical compression for strain up to (A) 14%, (B) 8 (red) and 5% (blue). (C) Secant modulus resulting from compression of a 3D PCL sample. The standard deviation refers to an average of 10 consecutive ramps.
Fig. 4: (A) Micro CT reconstruction of 3D PCL entire volume (B) SEM picture of the top surface of samples. Black arrows point at fibers which are fused together as consequence of the fabrication process. (C) Cross-sections of samples obtained by volume rendering.
Fig. 5: (A) stress\strain curve varying temperature at 25, 30 and 37°C; (B) apparent elastic modulus values depending on temperature.
Fig. 6: (A) viscoelastic relaxation of scaffolds tested by cyclic loading over 10 cycles, (B) Relaxation pattern of four different samples relaxed under constant displacement over 180 min (C) stress/strain curves showing the behaviour of the material for 10 consecutive compression ramps after undergoing relaxation.
Fig. 7: Effect of different heights and compression rates on the response of PDMS samples. The mechanical response of 2 mm height samples compressed at 1 μm/s (blue) and 10 μm/s (red) are compared to that of 10 mm samples compressed at 10 μm/s (green). Each condition was tested on three samples (A, B, C).
Fig. 8: (A) stress/strain curves (1-10) repositioning the same sample among compression ramps applied at 10 μm/s (B) Apparent elastic modulus of 3D PCL samples (A, B, C) tested varying the velocity of application of compressive ramps at 1 um/s (blue) and 10 um/s (red).
Fig. 9: boxplots to evaluate normality on samples with negative Shapiro test results. The boxes represent the distribution of data: the median is indicated by the bold black line dividing the box in 2 parts. Datas can be considered with a normal distribution if the line is in the middle of the box and the standard deviations are similar comparing the top and the bottom half. Values higher than 3/2 times the upper of lower quartile are considered outliers according to the outlier test performed automatically by SPSS. From left to right, graphs refer respectively to sample A compressed at 1 μm/s and sample B compressed at 10 μm/s.
Fig. 10: (A) Storage modulus, (B) loss modulus and (C) tan δ resulting from DMA analysis on 3D PCL samples tested in air (continuous line) or water (dot line). Statistical significant differences are marked by * (*$p<0.05$).

Fig. 1,1-column

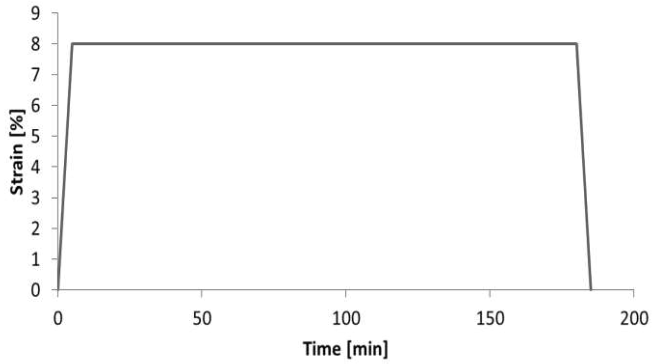

Fig. 2, 1-column

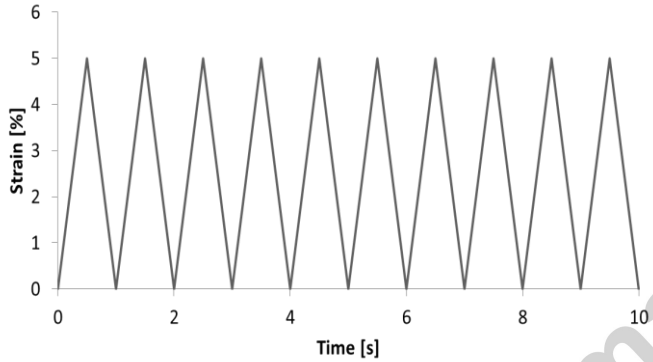

Fig. 3 single column

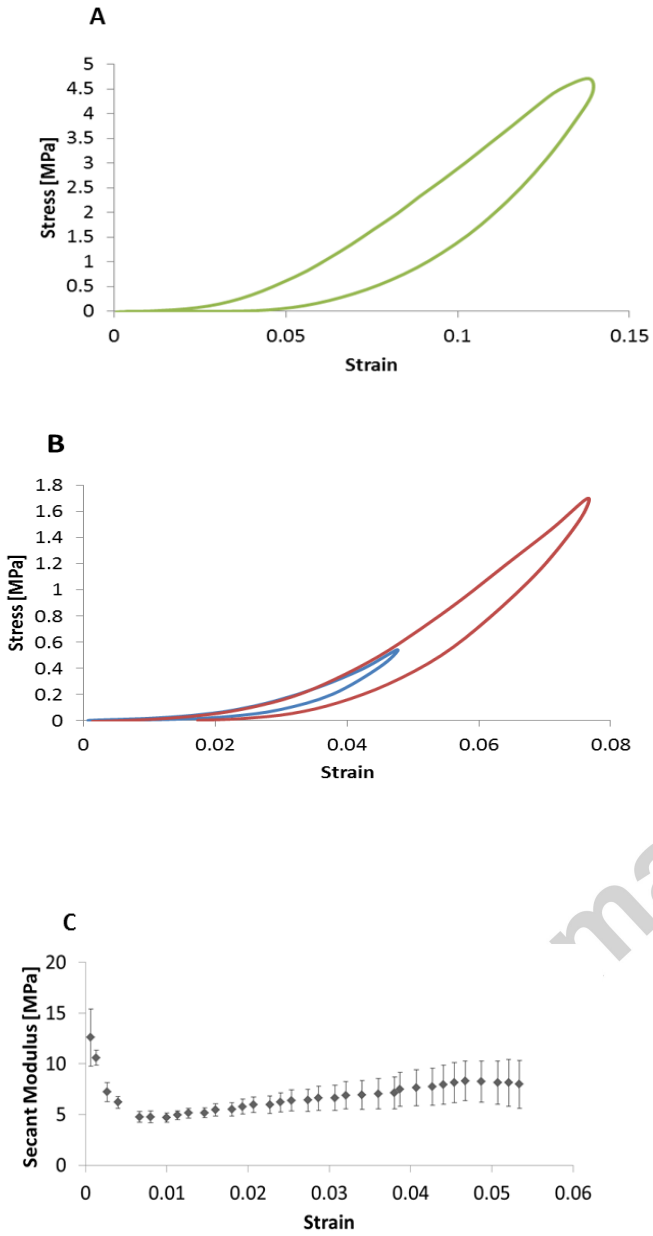

Fig. 4: double column

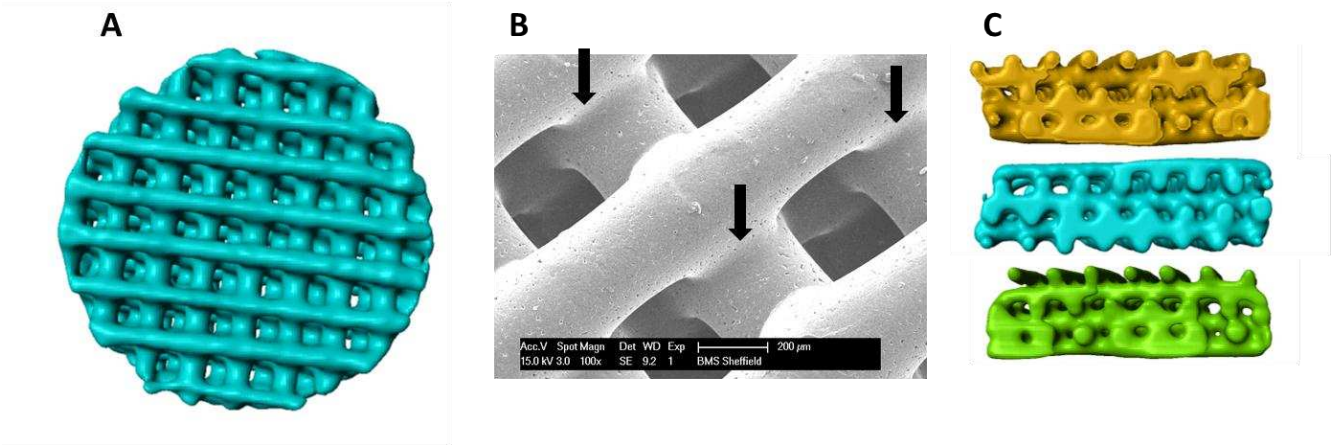

Fig. 5 single column

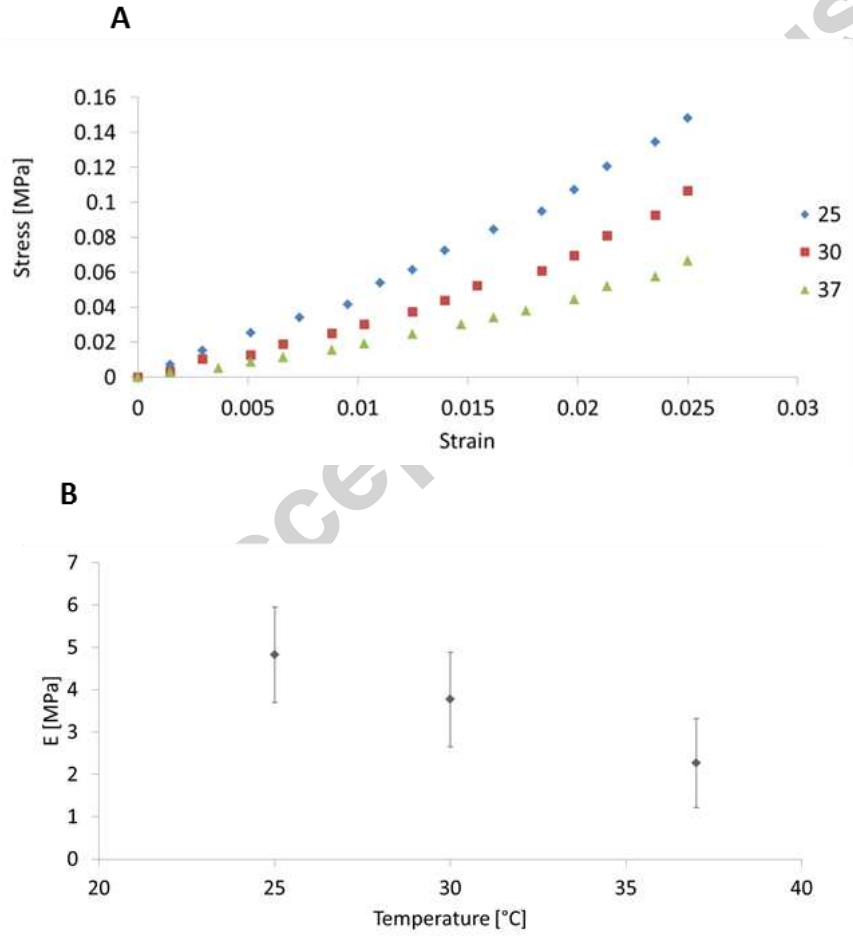

Fig. 6 single column

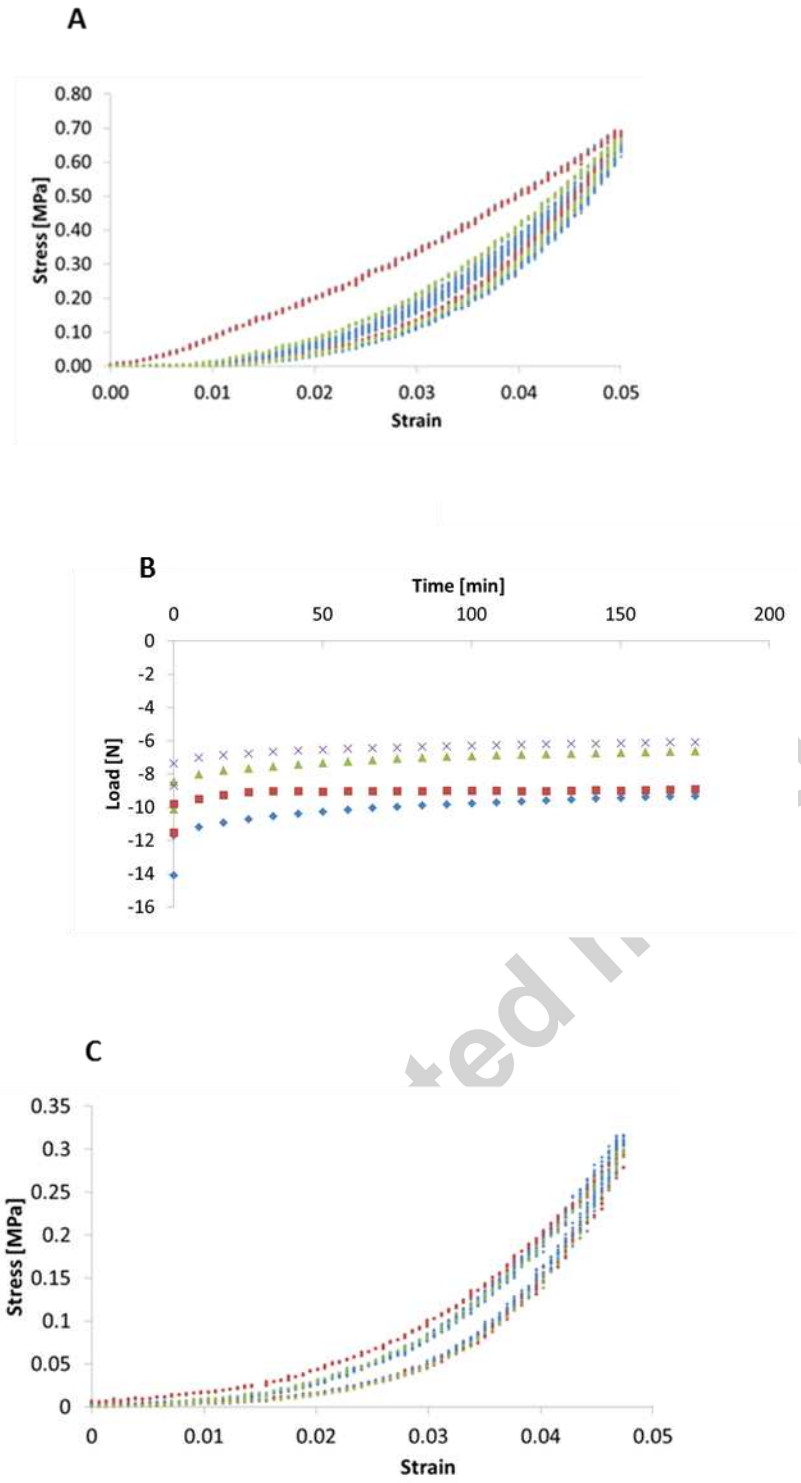

Fig. 7 single column

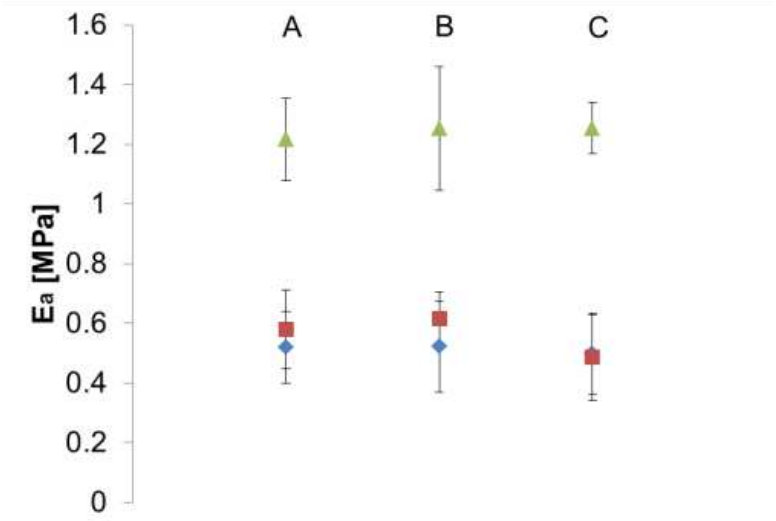

Fig. 8 single column

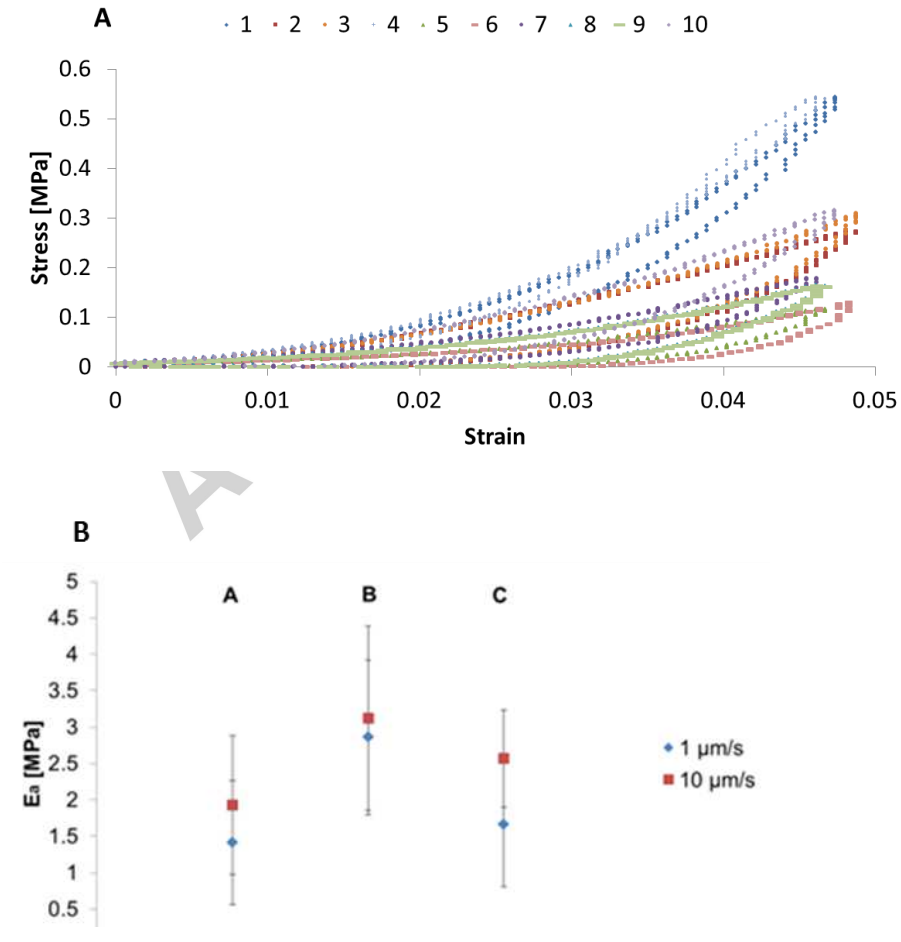

Fig. 9 1.5 column

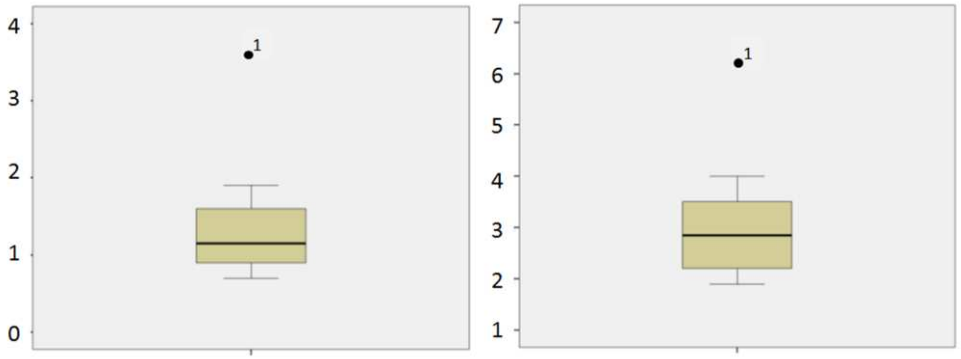

Fig. 10 1.5 column

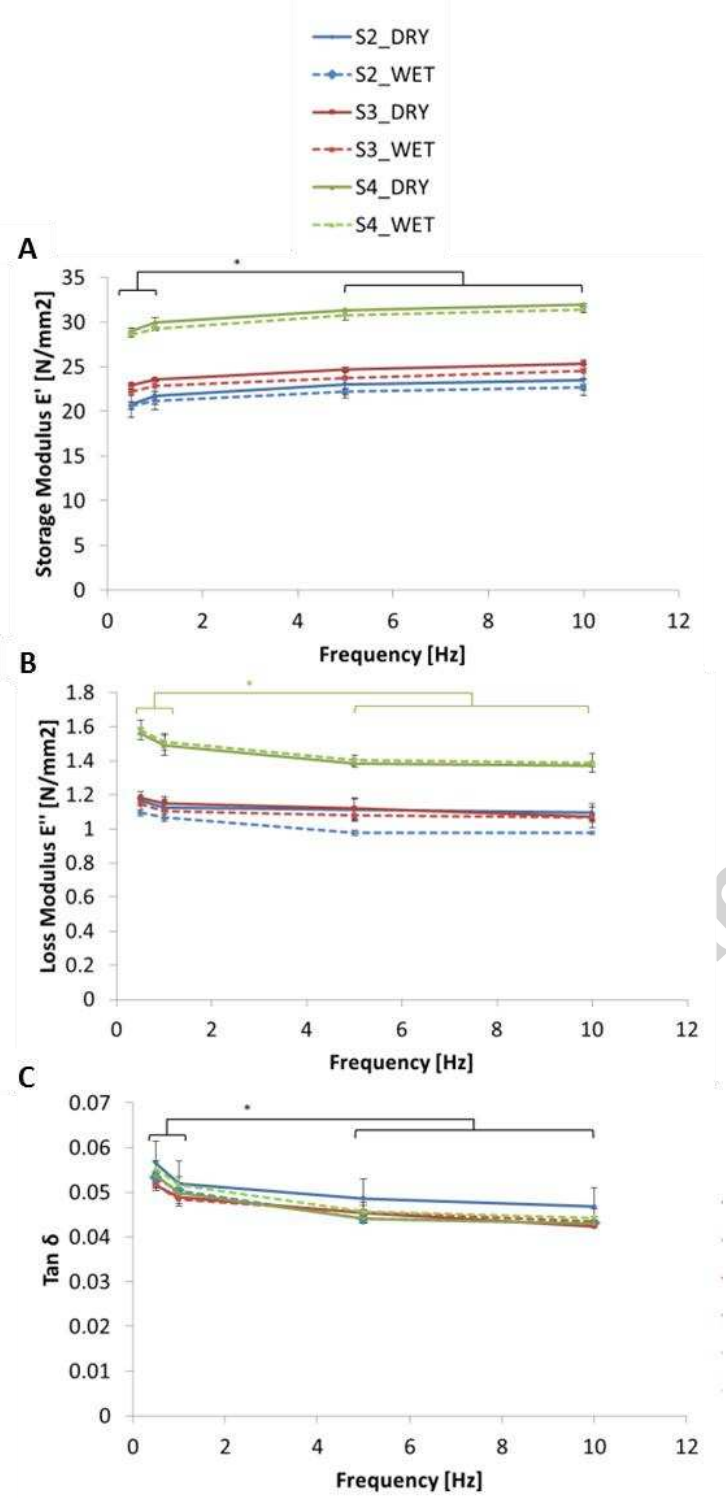

List of tables

8 Table 3: Geometrical parameters involved in the evaluation of 3D PCL geometrical variability.

9 Table 4: SPSS statistics of Ea data obtained compressing 10 times PDMS samples. Height was varied at 2 mm (PDMS2) and 10 mm (PDMS10). Series of data obtained by compression of each sample (A, B, C) are tested for normality. Levene's test is performed to confirm equality of variances among different samples presenting same geometry. Afterwards, ANOVA and T-Test are performed to confirm similarity in Ea values by employing respectively different samples with the same height or samples with different height. Eventually T-Test is further adopted to evaluate variability among single samples 2 mm height tested at different velocities.

10 Table 5: Shapiro tests normality on 3D PCL samples compressed at 1 mm/s and 10 mm/s; Levene and T Test respectively verify equality of variances and identify any significant difference among single samples compressed at different velocity.

11 Table 6: Tukey post-hoc test showing significant differences among Ea within different samples tested at 1 µm/s and 10 µm/s.

12 Table 7: Levene's test for equality of variances of samples (A, B, C) compressed at the same velocity.

13 Table 8: Comparison among the literature studies evaluating the stiffness of 3D PCL when molecular weight, dimensions, compression protocol, laydown pattern, porosity, pore size and surrounding environment are varied.

Table 9: Comparison of the literature studies testing the mechanical performance of 3D PCL.

Table 1

PCL SAMPLE	HEIGHT [mm]	POROSITY [%]
S2	1.37	42
S3	1.52	44
S4	1.54	45

Table 1

PCL SAMPLE	HEIGHT [mm]
A	1.54
B	1.61
C	1.39

Table 2

Sample number	Height [mm]	Surface area [mm2]	Volume [mm3]	Fiber diameter [µm]	Porosity [%]
1	1.42	137.67	13.04	290	31.6
2	1.36	145.91	13.31	254	46.54
3	1.62	148.59	12.59	305	46.61
4	1.52	145.94	13.31	284	43.74
5	1.55	153.04	15.88	348	34.2
6	1.67	155.68	16.76	393	50.9
7	1.61	201.12	15.95	335	48.25
8	1.61	166.03	13	380	47.73
9	1.59	159.31	17.84	335	42.71
10	1.55	147.22	13.56	315	35.5
11	1.66	161.91	12.51	300	40.3
12	1.53	151.22	12.14	299	36.09
13	1.67	157.17	13.28	296	35.5
14	1.53	122.66	13.28	296	51.2
Average	**1.56**	**153.82**	**14.03**	**316**	**42.2**
Standard deviation	**0.09**	**17.39**	**1.79**	**38**	**6.6**

Table 3

SAMPLE	TRIPLICATES	SHAPIRO TEST	LEVENE'S TEST	ANOVA	T-TEST	T-TEST VARYING VELOCITY
PDMS2	A	0.263	0.547	0.923	0.000	0.309
	B	0.575				0.113
	C	0.143				0.824
PDMS10	A	0.558	0.597	0.073		-
	B	0.802				
	C	0.599				

Table 4

PCL SAMPLE	VELOCITY [µm/s]	SHAPIRO TEST	LEVENE TEST	T TEST
A	1	0.003	0.404	0.215
	10	0.069		
B	1	0.473	0.770	0.624
	10	0.034		
C	1	0.093	0.343	0.016
	10	0.199		

Table 5

VELOCITY [µm/s]	TUKEY POST-HOC TEST		
	SAMPLES	A	B
1	B	0.010	-

10	C	0.792	0.032
	B	0.072	-
	C	0.221	0.462

Table 6

VELOCITY	SAMPLE	LEVENE'S TEST
1	A	0.752
	B	
	C	
10	A	0.485
	B	
	C	

Table 7

Study	Molecular weight	Dimensions [mm]	Compression protocol	Laydown pattern	Porosity [%]	Pores size [µm]	Surrounding environment	Stiffness [MPa]
Hutmacher	80,000	6.5 x 6.5 x 13.5	0.7% strain 16.7 µm/s (37°C)	0/60/120°	55	380 x 430 x 590	Air	41.9±3.5
							PBS	29.4±4.0
				0/72/144/36/108°	56	360 x 410 x 620	Air	20.2±1.7
							PBS	21.5±2.9
Yeo	115,000	3 mm height 5 mm diameter	80% strain 16.7 µm/s (27°C)	0/60/120°	70	-	Culture medium	23.1±6.2
Sobral	-	5 x 5 x 5	80% strain 33 µm/s (37°C)	0/90°	31	100	PBS	8±0.5
					81	750		1.5±0.2
					60	100-750-100		3±0.1
					56	750-100-750		3.5±0.5
Brunelli	43,000-50,000	1.5 mm height	5% strain 10 µm/s	0/90°	42	300	Air	2.2±1

	5 mm diameter	(37°C)						

Table 9

Study	Dimensions [mm]	Compression protocol	Laydown pattern	Porosity [%]	Pores size [µm]	Surrounding environment	Storage Modulus [MPa]	Tan δ
Sobral	5 x 5 x 5	1.4% strain	0/90°	31	100	PBS	8 MPa at 0.1 Hz increasing linearly up to 11 MPa at 10 Hz.	Values between 0.10 and 0.16 depending on the porosity and progressively decreasing for frequencies up to 0.5 Hz. It remains constant for higher frequency values.
				81	750		Similar values between 2 and 4 MPa depending on pore size. It remains constant with increasing frequency	
				60	100-750-100			
				56	750-100-750			
Yilgor	5 mm diameter	-	0/90	51	-	Air	18.5±0.2	0.05
			0/90 + offset	66			3.5±0.1	0.07
			0/45/90	65			11.5±0.1	0.05
			0/45/90 + offset	57			9.7±0.1	0.05

graphical

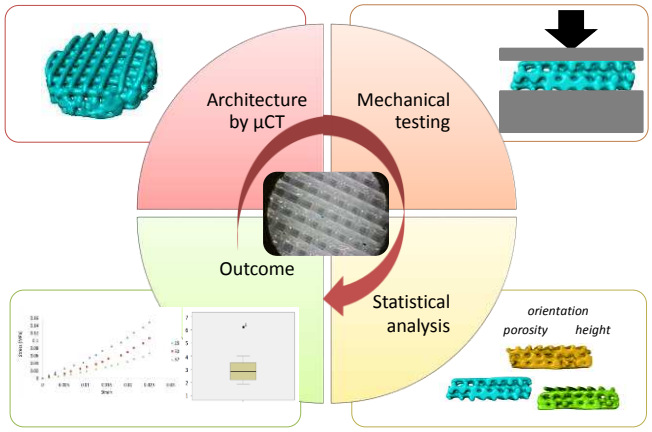

highlight

- 3D PCL responded linearly to compression for strains between 1 and 2.5%.
- Plastic deformation of 3D PCL was prevented applying compressive strains below 8%.
- A statistical analysis revealed a variability up to 30% in the mechanical response.